Proceedings of the 1st Marine Energy Technology Symposium
METS2013
April 10-11, 2013, Washington, D.C.

TIDAL TURBULENCE SPECTRA FROM A COMPLIANT MOORING

Jim Thomson*
NNMREC
University of Washington
Seattle, WA, USA

Levi Kilcher
Marine Hydrokinetics
National Renewable Energy Lab
Boulder, CO, USA

Marshall Richmond
Hydrology Group
Pacific Northwest National Lab
Richland, WA, USA

Joe Talbert
NNMREC
University of Washington
Seattle, WA, USA

Alex deKlerk
NNMREC
University of Washington
Seattle, WA, USA

Brian Polagye
NNMREC
University of Washington
Seattle, WA, USA

Maricarmen Guerra
Pontificia Universidad
Catolica de Chile
Santiago, Chile

Rodrigo Cienfuegos
Pontificia Universidad
Catolica de Chile
Santiago, Chile

ABSTRACT

A compliant mooring to collect high frequency turbulence data at a tidal energy site is evaluated in a series of short demonstration deployments. The Tidal Turbulence Mooring (TTM) improves upon recent bottom-mounted approaches by suspending Acoustic Doppler Velocimeters (ADVs) at mid-water depths (which are more relevant to tidal turbines). The ADV turbulence data are superior to Acoustic Doppler Current Profiler (ADCP) data, but are subject to motion contamination when suspended on a mooring in strong currents. In this demonstration, passive stabilization is shown to be sufficient for acquiring bulk statistics of the turbulence, without motion correction. With motion correction (post-processing), data quality is further improved. Results from two field sites are compared, and the differences are attributed to the generation of large eddies by headlands and sills.

INTRODUCTION

The safe and effective design of turbines to harness tidal current energy requires detailed knowledge of the inflow conditions, which include ambient turbulence (as opposed to wake turbulence). Recently, [1] reported on turbulence measurements from two tidal energy sites using bottom-mounted instruments. Here, that work is extended to instruments mounted on a compliant mooring. The compliant mooring approach has the potential to provide hub-height (typically 10 to 20 m above the seabed) measurements with higher precision than bottom-mounted instruments. In particular, bottom-mounted Acoustic Dopper Current Profilers (ADCPs) cannot resolve short temporal scales (because of Doppler noise) and cannot resolve short spatial scales (because of divergent acoustic beams, or "beam spread"). High precision instruments, such as Acoustic Doppler Velocimeters (ADVs) do not suffer these sampling limitations, however these must be moored at hub-height and thus may be contaminated by the motion of the mooring itself.

Multiple demonstration deployments are used to test strategies for data collection and motion correction, with an emphasis on statistical quantification of the turbulence. The key quantities of interest are the turbulence intensity (i.e., the fluctuations relative to the mean) and the turbulence spectra (i.e., the fluctuations partitioned by frequency). Previous work has shown turbulence to be broadly partitioned between large-scale horizontal eddies, which contain most of the energy and thus control the turbulence intensity metric I, and smaller-scale isotropic eddies, which determine the dissipation rate ε of an energy cascade [2–8].

Here, analysis focuses on the horizontal magnitude of the currents (i.e., stream-wise speed), in order to maintain consistency with wind power meteorology. This is also a practical limitation of a passive yaw mooring, from which the primary

*Corresponding Author: jthomson@apl.uw.edu

TABLE 1. TTM deployments and sites

Deployment	Date	Site	Depth	TTM version	Max current
1	June 2012	Admiralty Head	56 m	3 vanes	2.1 m/s
2	Sep 2012	Admiralty Head	56 m	1 vane	2.4 m/s
3	Feb 2013	Chacao Channel	38 m	1 vane	3.0 m/s

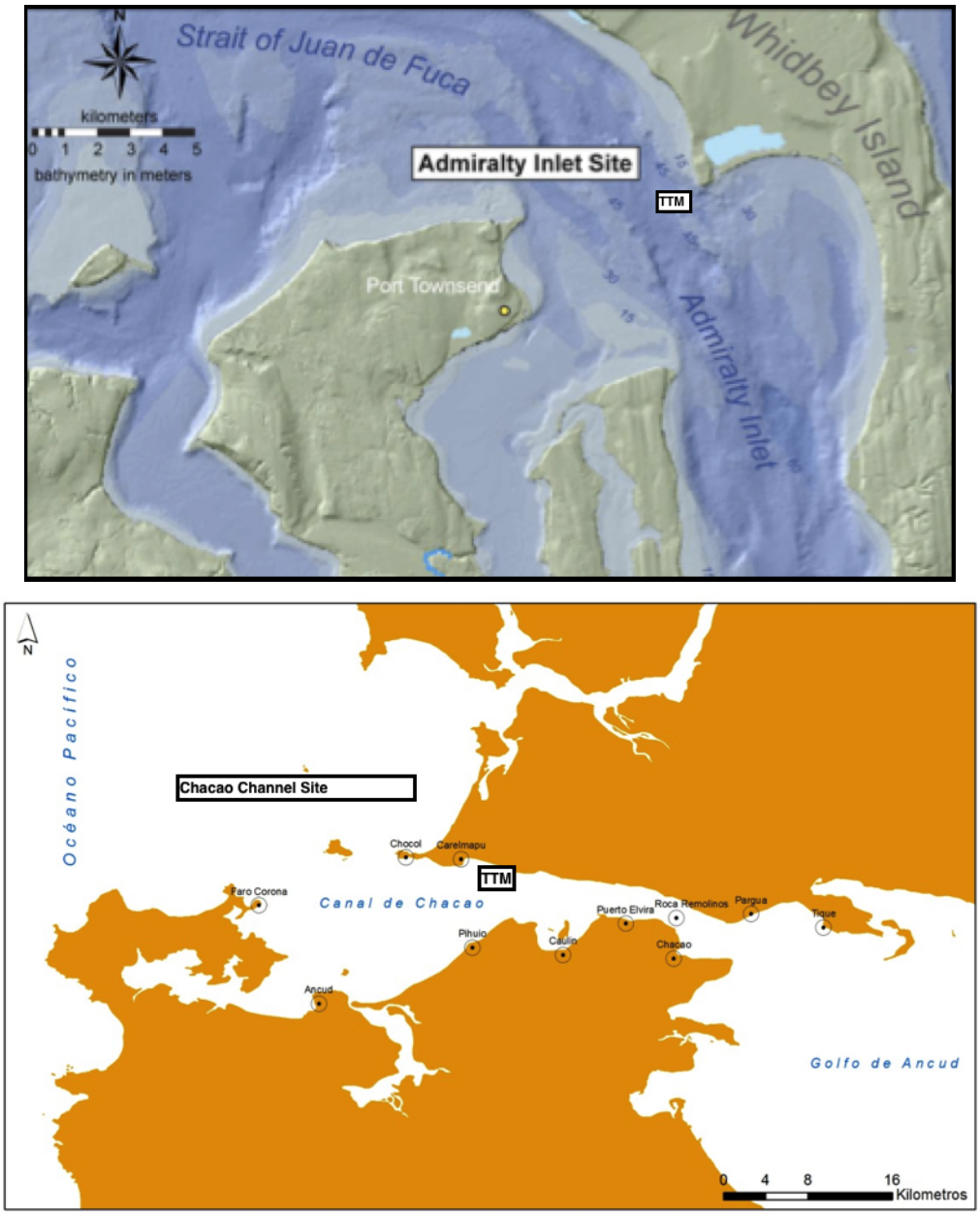

FIGURE 1. Admiralty Inlet in Washington State, USA (top) and Chacao Channel in Chiloe, Chile (bottom).

measurement is always the stream-wise component. It is important to note that the variance of orthogonal components (a more common oceanographic description of turbulence) is larger than the variance of scalar speed. Higher-order moments, such as the skewness, kurtosis, and extreme values are not addressed here.

DATA COLLECTION

To date, the Tidal Turbulence Mooring (TTM) has been deployed three times: twice in Admiralty Inlet (Puget Sound, WA, USA) in 2012, and once in Chacao Channel (Chiloe, Chile) in 2013. The deployments and sites are summarized in Table 1 and site plan views are shown in Figure 1. Each deployment was only a few days in duration, because the tidal harmonic characterization of these sites has already been conducted using multi-month deployments (e.g. [9]).

Site descriptions

The first deployment was from 17:30 PDT on 12 Jun 2012 to 14:30 PDT on 14 Jun 2012 at N 48 09.171', W 122 41.149' near Admiralty Head, Puget Sound WA (USA). The site is approximately 56 m deep (rel. MLLW) and the TTM deployment target depth was the nominal 10-m hub height of the Open Hydro turbines (2 total) that are planned to be deployed nearby in 2014, as a pilot project by Snohomish Public Utility District. The TTM deployment was within 10 m, horizontally, of the sea-spider deployment for the turbulence measurements in [1]. A second deployment from 12:45 PDT on 19 Sep 2012 to 14:45 on 20 Sep 2012 was conducted to assess the quality of passive acoustic (hydrophone) data collection as another potentional use of the TTM.

The third deployment was from 14:30 on 11 Feb 2013 to 10:00 on 14 Feb 2013 at S 41 45.746' W 73 40.949' near Carelmapu in the Chacao Channel, Chile. The site is approximately 38 m deep (rel. MLLW) and the TTM deployment targeted the nominal 10-m hub height of an Open Hydro turbine (for consistency with the Admiralty measurements).

Mooring description

Two versions of the TTM mooring are shown in Fig. 2, where the railroad (RR) wheel anchor is at the seabed and vertical distances z are upwards from the seabed. The mooring has no surface signature; the overall length is only that sufficient to achieve the desired hub-height. The overall concept is to use a heavy weight anchor (approx 2300 lbs) to hold the mooring in place laterally, and substantial buoyancy (approx 700 lbs) to hold the mooring nearly vertical. Instruments can then be deployed in-line on the mooring and measure turbulent flows at turbine hub-heights. The mooring line is wrapped with filaments to reduce strumming. The instruments are mounted to vanes with swivels, and the intent is for the instruments to point (yaw) into the flow under all conditions (i.e., flood and ebb). This free yaw defines a local right-handed coordinate system in which $+\hat{x}_{TTM}$ is into the flow, $+\hat{y}_{TTM}$ is across the flow, and $+\hat{z}_{TTM}$ is vertically up.

Instruments and sampling parameters

The instruments and sampling parameters from the first TTM deployment are given in Table 2, listed from the seabed upwards. Each mooring element includes an orientation sensor to provide the yaw direction in post-processing and address motion contamination. All mooring components are nonferrous, except the RR wheels at the bottom, to avoid contamination of magnetometer heading measurements. In addition, conductivity-temperature-depth (CTD) measurements were collected $z = 0.72$ and 14.2 m above seabed with SBE 37s, but these are not listed in the table.

The Nortek Vector ADVs (3 total) sampled velocity at 32 Hz in the local XYZ coordinate system. The nominal velocity range was set conservatively at 4 m/s, which is equivalent to 5 m/s horizontal and 1 m/s vertical). This choice was to ensure good data even in the case of extreme mooring angles, when the "vertical" measurement would be approaching the expected horizontal magnitudes of 2 m/s. The ADVs also sampled pressure at 32 Hz. During the Chacao deployment, this was reduced to 16 Hz sampling with a 2 m/s nominal velocity range (= 3.5 horizontal range) with a goal of reducing Doppler noise in the measurements.

The ADVs were mounted to vanes such that the sampling volume (approximately 0.01 m diameter, located 0.15 m above or below the sensor) is clear of any upstream obstruction, and downstream is only the mooring line (as opposed to the vane assembly). The mooring line is 1/2" (=0.013 m) diameter, and the sampling volume is 0.24 m upstream of the line. Using the common rule of 10 diameters, the mooring line is not expected to contaminate the measurement. The motion sensors for each ADV are in the electronics cases, which are mounted 0.24 m downstream of the center line. Thus, the total offset is $\Delta x = +0.48$ m and rotation measured about the mooring axis should be symmetric between the sampling volume and the motion sensor. The NREL ADV had Microstrain 3DM-GX3 motion sensor with synchronous data acquisition (integration by Nortek). The APLUW and PNNL ADVs had x-IMU motions sensors with asynchronous data (independent SD card). The asynchronous data are within 1 sec of the velocity data, based on NTP comparisons in bench testing.

An Inter-Ocean S4A electromagnetic (EM) current meter also was include in the first deployment. This sampled horizontal currents at 2 Hz, with onboard corrections for tilt and heading. The S4A also recorded CTD measurements.

An Acoustic Wave And Current Profiler (AWAC) was deployed on the RR wheel anchor and collected current profiles every 1 s at 1 m resolution from 1.1 to 20.1 m above the seabed. The resulting AWAC Doppler noise of 0.112 m/s must be removed

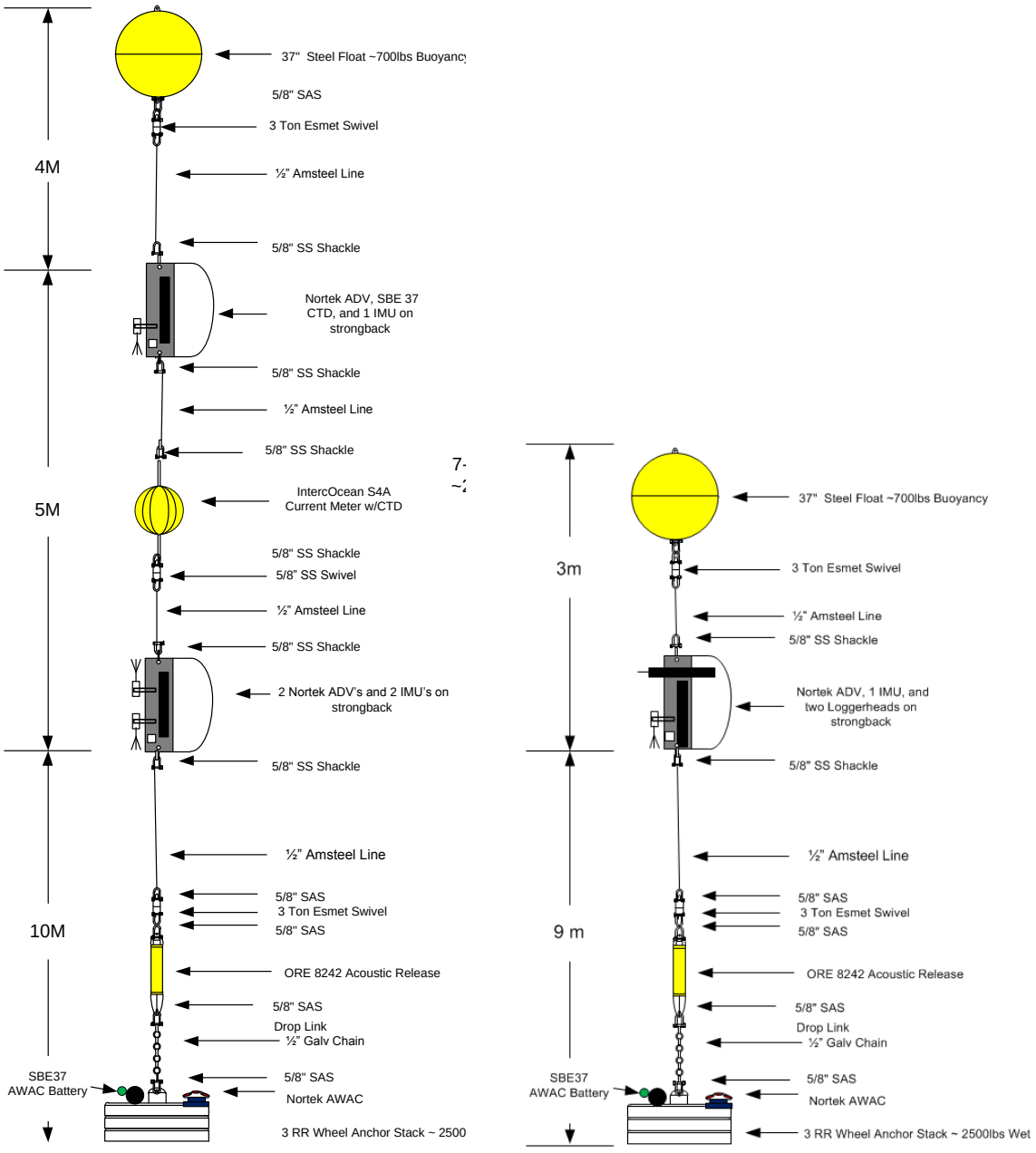

FIGURE 2. Dimensional drawings of Tidal Turbulence Moorings deployed in Admiralty Inlet (left) and Chacao Channel (right).

from statistical descriptions of the turbulence (see [1]). The AWAC recorded velocities in a magnetic East-North-Up (ENU) coordinate frame, using the standard onboard compass heading. Since the RR wheels are common steel, the compass heading output may be biased, and resulting current directions must be validated against previous measurements at the site. Another data quality concern is the potential interference of the upper mooring elements, which may intersect the AWAC beams during large mooring angles. (When the mooring is purely vertical, under slack conditions, the beam divergence of 25° has sufficient clearance with the mooring elements).

TABLE 2. TTM instruments, positions, and sampling parameters during the June 2012 deployment in Admiralty Inlet. Other deployments used a simplified single-vane version, with two Loggerhead hydrophones added to the vane.

Instrument	Nortek AWAC	Nortek Vector	Nortek Vector	InterOcean S4A	Nortek Vector
Type	Uplooking Profiler	ADV	ADV	Electormagnetic	ADV
Owner	APL-UW	APL-UW	NREL	OARS	PNNL
Height $z_{\alpha=0^\circ}$ [m]	1.1-20.1	10	11	12.5	14
Height $z_{\alpha=20^\circ}$ [m]	1.1-20.1	9.4	10.3	11.7	13.1
Sampling frequency [Hz]	1	32	32	2	32
Sampling diameter [m]	1+	0.01	0.01	0.3	0.01
Motion sensor	onboard	x-IMU	Microstrain 3DM-GX3	onboard	x-IMU
Coordinate system	ENU	XYZ (down)	XYZ* (up)	EN	XYZ (down)
Offset Δx [m]	n/a	+0.48	+0.48	n/a	+0.48
Offset Δy [m]	n/a	-0.03	+0.07	n/a	-0.03
Offset Δz [m]	n/a	-0.8	+0.27	n/a	-0.8

The Microstrain (MS) is mounted such that $\hat{x}_{TTM} = \hat{y}_{MS}$, $\hat{z}_{TTM} = \hat{x}_{MS}$, $\hat{y}_{TTM} = \hat{z}_{MS}$,

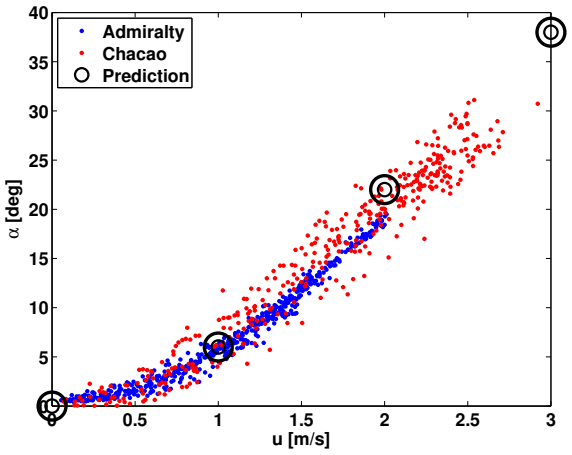

FIGURE 3. Predicted and observed mooring angles versus observed flow speeds. Blue points are from Admiralty Inlet (deployment 1), red points at from Chacao Channel (deployment 3), and black circles are predictions from mooring simulations.

ANALYSIS

Mooring performance

The demonstration deployments have been used to assess the stability of the TTM design. The TTM successfully holds position (confirmed via ship's GPS on deployment and recovery) during the deployment. The orientation sensor on the AWAC during the first deployment indicated that RR wheel anchor pitched about 10° at the onset of the first tidal cycle, then remained stable. This is consistent with previous deployments of anchors and tripods at sites with strong flows.

The primary metric to assess mooring performance is the blow-down angle α (relative to vertical), which results from hydrodynamic drag in the strong currents. Simulations using Matlab Mooring Dynamics (MMD, open-source code from U. Victoria) predicted a 'blow-down' angle $\alpha \approx 22^\circ$ (relative to vertical) during uniform 2 m/s flow and $\alpha \approx 38^\circ$ during uniform 3 m/s flow. As shown in Figure 3, these predictions are consistent with the measurements of ADV pitch angle during the deployments.

Quality Control and burst statistics

Raw ADV data are quality controlled using a correlation cutoff (Elgar, 2001) [10] and despiked using a 3D phase space algorithm [11, 12]. Bad points are assigned NaN values and ignored in further processing. For the Admiralty deployments, these points are less than 1% of the dataset. For the Chacao deployment, velocity spikes are more common, comprising up to 10% of the points. With such a large number of bad points, quality control is essential prior to statistical analysis of the flows. Velocity spikes are expected in ADV data, however the relative difference in spike occurrence between sites remains unexplained.

Raw AWAC are quality controlled using the backscatter (echo) amplitudes. Under strong ebbs, reflections from mooring elements are clearly present as echo amplitudes exceeding 240 counts (uncalibrated). These points are less than 5% of the data set and are assigned NaN values.

Velocity data are processed in five-minute bursts, following [1], such that stationarity is achieved and the changes in the

tide do not affect the variance of the burst. Turbulence intensities are calculated from the stream-wise velocity component using the ratio of velocity standard deviation σ_u to velocity mean $\bar{u}$. Doppler noise removal is negligible for ADV data. (This is in contrast to ADCP or AWAC data, in which Doppler noise removal is essential.) Turbulence spectra are calculated using the FFT of 128 s windows which are tapered with a Hamming window, overlapped 50%, and then merged to obtain spectra with 12 degrees of freedom. Later, these spectra are binned by mean velocity to obtain characteristic spectra with approximately 96 degrees of freedom each.

Motion correction

Motion correction for the ADV data requires accurate measurements of mooring accelerations $\vec{a}$ and spatial translation from the location of the motion sensor to the velocity $\vec{u}$ sampling volume (see offsets in Table 2). Motion correction can be done directly for every point in a time series, or it can be done statistically using frequency spectra. Here, we focus on horizontal motions along the principal axis of the tidal flows ($-\hat{x}$, in the mooring reference frame, which yaws to face the mean current on ebb and flood). First, an initial correction is made, based on burst-averaged mooring angle α, to obtain an approximately horizontally stream-wise velocity u. Then, correction for variations in mooring orientation are applied.

Direct motion correction requires coherent (synchronous) data acquisition between raw velocity measurements u_{raw}, mooring accelerations a, and mooring rotation ω, such that true velocities in the mooring reference frame (facing the flow) can be obtained at every time step t via displacement and rotation:

$$\vec{u}(t) = \vec{u}_{ADV} + \vec{\omega} \times \vec{l} + \int \vec{a} \cdot dt, \qquad (1)$$

where $\vec{l}$ is the offset between the motion measurement and the velocity measurement.

Spectral motion correction, by contrast, is statistical. Since acceleration is $a = \frac{du}{dt}$ and frequency is $f = \frac{d}{dt}$, the contamination of motion (mooring accelerations) from turbulence frequency spectra can be removed via

$$TKE(f) = S_{uu} \quad \pm \quad 2X_{au} f^{-1} \quad - \quad S_{aa} f^{-2} \qquad (2)$$

where the analysis is restricted to the principal axis ($\hat{x}$). S_{uu} and S_{aa} are the auto-spectra of the ADV data and the accelerations, respectively, and the cross-spectra term X_{au} arises because mooring motion and raw velocity observations are not independent. Rather, velocities are correlated with mooring motion. This is particularly important at low frequencies, where large velocity anomalies cause the mooring to blow-down and thus a decreases as the ADV measured u decreases. This implies phase is important (to set the sign of X), and thus motion and velocity measurements must be at least quasi-synchronous.

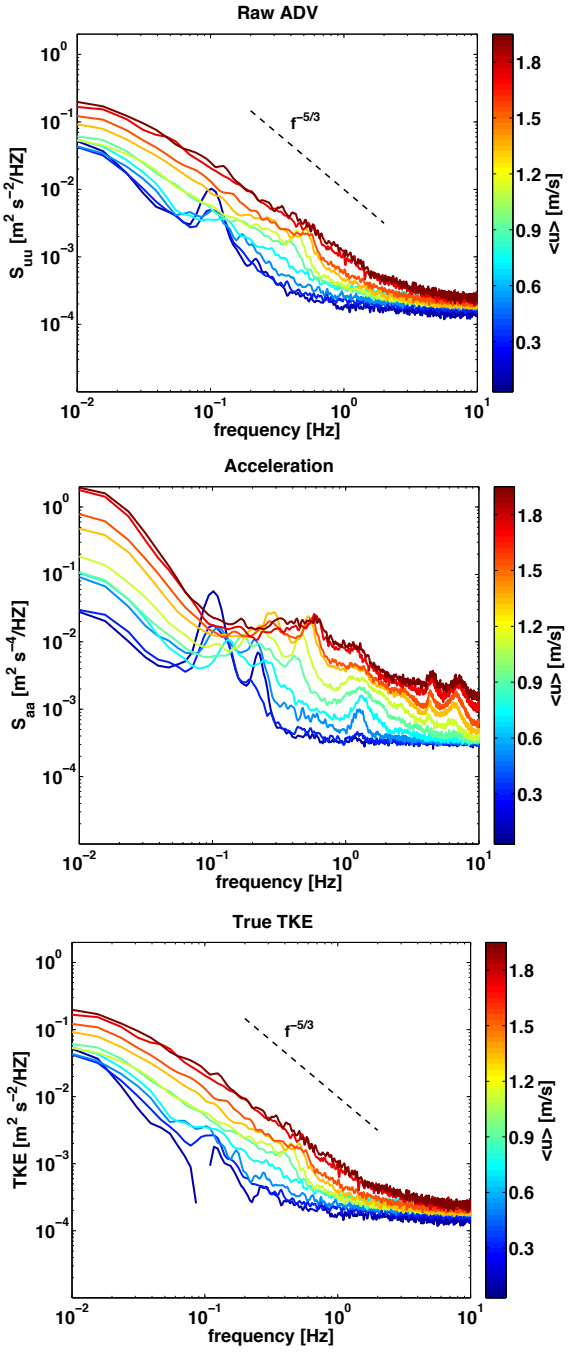

FIGURE 4. Raw TKE spectra (top), acceleration spectra (middle), and corrected TKE spectra (bottom).

Figure 4 shows the raw TKE spectra, the acceleration spectra, and the corrected TKE spectra. The raw TKE spectra have

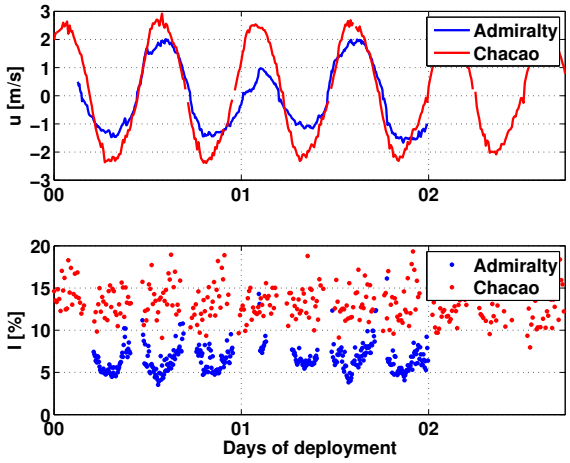

FIGURE 5. Times series of five-minute mean speeds (top panel) and turbulence intensity (lower panel).

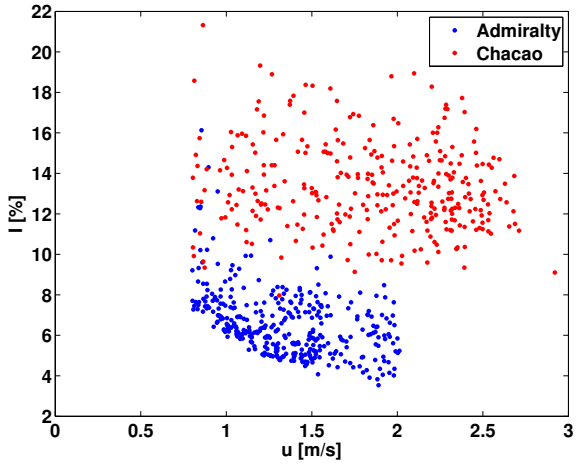

FIGURE 6. Turbulence intensity as a function of mean velocity.

peaks correlated with peaks in the acceleration spectra which are consistent with low-mode mooring oscillations that increase with flow speed (i.e., $f = \frac{u}{L}$ where L is the mooring length). These peaks are largely absent from corrected TKE spectra. TKE spectra calculated from the direction motion-corrected data (not shown) are similar to the results from the spectral motion correction. Direct motion correction, however, has the advantage of preserving time-domain information from the flow, which can then be used to assess coherence and higher-order statistics.

Both the raw spectra and the acceleration spectra show evidence of a resonant mode in the mooring dynamics, which increases in frequency with increasing mean current (from 0.1 Hz at 0.3 m/s to 1 Hz and higher to 1.8 m/s). This resonant mode represents the most severe motion contamination, though it becomes weak compared with the observed turbulence at the higher speeds relevant to turbines (i.e., greater than 1 m/s).

RESULTS

Turbulence Intensities

The basic statistics observed during the TTM deployments are largely consistent with the results of previous work. The mean flows are largely harmonic, and the turbulence intensities $I = \frac{\sigma_u}{\bar{u}}$ range from 5 to 20%. However, as shown in time series of Figure 5, there are notable differences in the patterns of the turbulence. In Figure 6, the Admiralty data have a mild trend of decreasing I with increasing mean velocity u, but the Chacao data have no trend. This may be related to the larger flows at Chacao, which must change more rapidly within a tidal cycle, or it may be related to the geometry of the channels.

Spectra

Turbulence spectra, $S_{uu}(f)$ also are consistent with previous results, including regions of anisotropic eddies (at low frequencies), an isotropic inertial range (a mid frequencies), and Doppler noise (at high frequencies). As shown in Figure 4, the spectra are well sorted by mean velocity, consistent with the result from the quasi-constant turbulence intensity metric (since this metric is a ratio, constant values require the turbulence to increase when the mean velocity increases).

Figure 7 shows averaged and normalized spectra, in which the transition from two-dimensional horizontal turbulence to three-dimensional isotropic turbulence occurs at approximately the shear frequency, $f_s \approx \frac{du}{dz}$. The isotropic frequencies follow the expected $f^{-5/3}$ dependence [13]. The spectra are far more energetic at Chacao, where the mean velocities and turbulence intensities are also greater. Even when normalized by the mean kinetic energy u^2 and the shear frequency, f_s, Chacao remains elevated relative to Admiralty. When normalized by the total streamwise turbulent kinetic energy σ_u^2 and the shear frequency, f_s, the spectra converge in the isotropic range. At lower frequencies, however, Chacao remains elevated relative to Admiralty. This may be related to the different mechanisms for turbulence generation at larger scales, such as headlands (e.g., [14]), which set the amplitude in a cascade of energy from low frequencies to high frequencies. Thus, the isotropic ranges are similar only when normalized by the total turbulent kinetic energy. This is consistent with an expectation for the turbulence dynamics to be universal across different sites, but for the turbulence intensity to be site-specific.

Dissipation rates

The cascade of energy in the isotropic frequency range is related to the dissipation rate of turbulent kinetic energy. Much

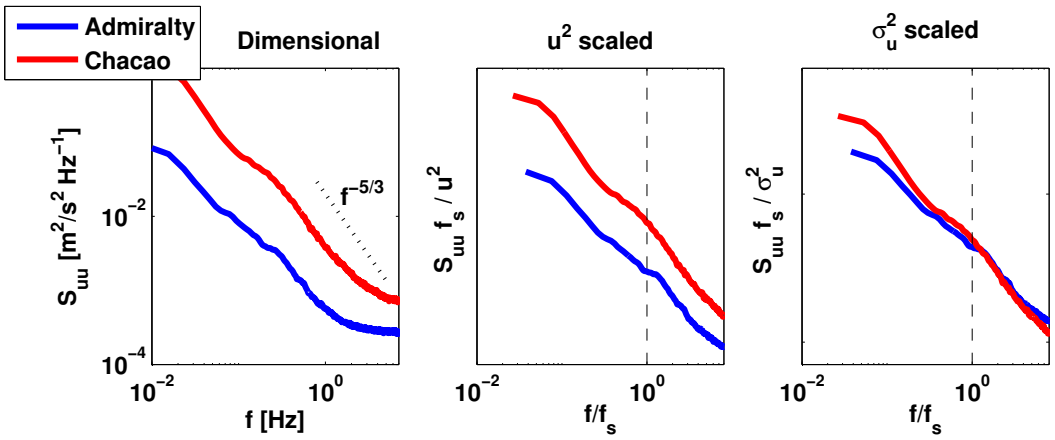

FIGURE 7. Average turbulent kinetic energy density versus frequency from ADV measurements at approximately 10 m above the seabed. Dimensional (left) and scaled by mean velocity and shear frequency (middle, right). The dotted line in the left panel shows the expected dependence of an isotropic energy cascade. The dashed lines in the middle and right panels indicate the shear frequency f_s, where a transition from horizontal to isotropic eddies is expected. Averages exclude tidal currents less than 1 m/s, which are below the nominal cut-in speed of tidal turbines.

as the turbulence intensity can be considered a scalar measure of the large-scale portion of a turbulence spectrum, the dissipation rate ε is measure of the amplitude in the smaller-scale isotropic portion of the spectrum. It is determined by [15]

$$S_{ww}(f) = a\varepsilon^{2/3} f^{-5/3} \left(\frac{\bar{u}}{2\pi}\right)^{2/3}, \qquad (3)$$

where a is a constant taken to be 0.69 for the vertical spectra. Similar to the turbulence intensity, this metric is uniformly larger at Chacao Channel, even at the same mean velocity.

Figure 8 shows a strong relationship between the mean velocity and the dissipation rate. The dissipation rate follows the theoretical scaling of $\frac{u^3}{l}$ from [13], where l is a characteristic length scale (nominally the depth). This indicates that spectral scaling by velocity is consistent within each data set (i.e., at each location), but differs between them. Again, the difference is likely driven by the large scale generation mechanisms, which are unique to the bathymetry of each location.

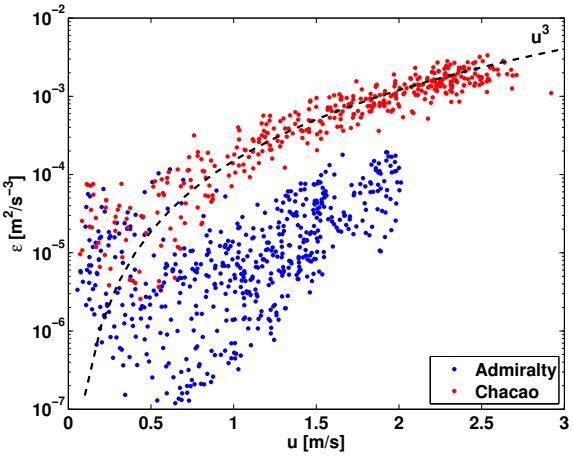

FIGURE 8. Turbulent dissipation rate as a function of mean velocity. The dashed lines shows the theoretical u^3 scaling.

CONCLUSIONS

Compliant moorings are a promising approach to collecting turbulence data at tidal energy sites. Raw results show clearly the benefits of careful mooring design. Indeed, the best motion correction may be motion prevention. Although there is notable motion contamination, the raw data are sufficiently 'clean' to obtain consistent turbulence intensities and reasonable turbulence spectra, especially above 1 m/s cut-in speeds. Motion correction is required, however, to examine the more detailed aspects of the turbulence (i.e., higher moments and coherence).

In comparing results from Admiralty Inlet and Chacao Channel, there is more turbulence at Chacao Channel. This elevated turbulence is thought to be produced at large scales is attributed to the bathymetry and headlands of each site.

ACKNOWLEDGMENT

Thanks to Capt. Andy Reay-Ellers ship operations in Admiralty Inlet and Eduardo Hernandez for ship operations in Chacao. Thanks to Chris Bassett for the addition of passive acoustics to the moorings. Support for this research provided by the U.S. Department of Energy and by the Office of Naval Research - Global.

REFERENCES

[1] Thomson, J., Polagye, B., Durgesh, V., and Richmond, M., 2012. "Measurements of turbulence at two tidal energy sites in Puget Sound, WA". *J. Ocean. Eng.,* ***37***(3), pp. 363–374.

[2] Lu, Y., and Lueck, R. G., 1999. "Using a broadband ADCP in a tidal channel. part ii: Turbulence". *J. Atmos. Ocean. Tech.,* ***16***, pp. 1568–1579.

[3] Stacey, M. T., Monismith, S. G., and Burau, J. R., 1999. "Observations of turbulence in a partially stratified estuary". *J. Phys. Oceanogr.,* ***29***, pp. 1950–1970.

[4] Stacey, M., 2003. "Estimation of diffusive transport of turbulent kinetic energy from acoustic Doppler current profiler data". *J. Atmos. Ocean. Tech.,* ***20***, pp. 927–935.

[5] Rippeth, T. P., Simpson, J. H., Williams, E., and Inall, M. E., 2003. "Measurements of the rates of production and dissipation of turbulent kinetic energy in an energetic tidal flow: Red Warf Bay revisited.". *J. Phys. Oceanogr.,* ***33***, pp. 1889–1901.

[6] Williams, E., and Simpson, J. H., 2004. "Uncertainties in estimates of Reynolds stress and TKE production rate using the adcp variance method". *J. Atmos. Ocean. Tech.,* ***21***, pp. 347–357.

[7] Wiles, P., Rippeth, T. P., Simpson, J., and Hendricks, P., 2006. "A novel technique for measuring the rate of turbulent dissipation in the marine environment". *Geophys. Res. Let.,* ***33***, p. L21608.

[8] Walter, R. K., Nidzieko, N. J., and Monismith, S. G., 2011. "Similarity scaling of turbulence spectra and cospectra in a shallow tidal flow". *J. Geophys. Res.,* ***116***(C10019).

[9] Polagye, B., and Thomson, J., 2013. "Tidal energy resource characterization: methodolgy and field study in Admiralty Inlet, Puget Sound, USA". *Proc. IMechE, Part A: J. Power and Energy*.

[10] Elgar, S., Raubenheimer, B., and Guza, R. T., 2001. "Current meter performance in the surf zone". *J. Atmos. Ocean. Tech.,* ***18***, pp. 1735–1746.

[11] Goring, D. G., and Nikora, V. I., 2002. "Despiking acoustic doppler velocimeter data". *J. Hydraul. Eng,* ***128***(1), pp. 117–126.

[12] Mori, N., Suzuki, T., and Kakuno, S., 2007. "Noise of acoustic doppler velocimeter data in bubbly flow". *ASCE Journal of Engineering Mechanics,* ***133***(1), pp. 122–125.

[13] Kolmogorov, A. N., 1941. "Dissipation of energy in the locally isotropic turbulence". *Dokl. Akad. Nauk SSR,* ***30***, pp. 301–305.

[14] Signell, R. P., and Geyer, W. R., 1991. "Transient eddy formation around headlands". *J. Geophys. Res.,* ***96***(C2), pp. 2561–2575.

[15] Lumley, J. L., and Terray, E. A., 1983. "Kinematics of turbulence convected by a random wave field". *J. Phys. Oceanogr.,* ***13***, pp. 2000–2007.